

Quantum States of Neutrons in Magnetic Thin Films

F. Radu^{1,*}, V. Leiner², M. Wolff^{1,3}, V. K. Ignatovich⁴, and H. Zabel¹

¹Department of Physics, Ruhr-University Bochum, D- 44780 Bochum, Germany

²Institut für Werkstoffforschung WFN, GKSS Forschungszentrum GmbH, 21502 Geesthacht, Germany

³Institut Laue-Langevin, F-38042 Grenoble Cedex 9, France and

⁴Frank Laboratory of Neutron Physics, Joint Institute for Nuclear Research, 141980, Dubna Moscow Region, Russia

(Dated: November 17, 2017)

We have studied experimentally and theoretically the interaction of polarized neutrons with magnetic thin films and magnetic multilayers. In particular, we have analyzed the behavior of the critical edges for total external reflection in both cases. For a single film we have observed experimentally and theoretically a simple behavior: the critical edges remain fixed and the intensity varies according to the angle between the polarization axis and the magnetization vector inside the film. For the multilayer case we find that the critical edges for spin up and spin down polarized neutrons move towards each other as a function of the angle between the magnetization vectors in adjacent ferromagnetic films. Although the results for multilayers and single thick layers appear to be different, in fact the same spinor method explains both results. An interpretation of the critical edges behavior for the multilayers as a superposition of ferromagnetic and antiferromagnetic states is given.

PACS numbers: 74.78.Fk, 61.12.Ex, 75.25.+z

Keywords: Magnetic multilayers, polarized neutron scattering

INTRODUCTION

Neutron reflectivity goes back to 1946 when it was first used by Fermi and Zinn for the determination of coherent scattering lengths [1]. Subsequently inserting a polarizer and analyzer to produce a polarized neutron beam, Hughes and Burgoyne started to perform polarized neutron experiments as early as 1951 [2]. It was foreseen by the authors of this work that *beams of completely polarized neutrons will be useful in the study of magnetic and nuclear properties*. The next major achievement of Polarized Neutron Reflectometry (PNR) was the prediction of spin-flip reflectivity by Ignatovich (1978) [3] and the pioneering experiments on magnetic surfaces by Felcher (1981) [4]. While specular PNR is widely recognized as a powerful tool for the investigation of magnetization profiles in magnetic heterostructures [5], the description of off-specular scattering from magnetic domains is still under development [8]. In spite of these important developments there is still a confusion concerning the quantum states of neutrons in a magnetic sample. Here we show unambiguously that the neutron has to be treated as a spin 1/2 particle [6, 7] in each homogeneous magnetic layer. This is at variance with the conventional description of neutron reflectivity, which often considers the neutron magnetic potential as a classical dot product [9, 10, 11, 12].

Neutrons interact with a magnetic thin film via the Fermi nuclear potential and via the magnetic induction. Thus, the neutron - film interaction hamiltonian includes both contributions: $V = V_n + V_m = (\hbar^2/2m)4\pi Nb - \boldsymbol{\mu} \cdot \mathbf{B}$, where m is the neutron mass, N is the particle density of the material, b is the coherent scattering length, $|\boldsymbol{\mu}|$ is the magnetic moment of the neutron, and $|\mathbf{B}|$ is the magnetic induction of the film. Unconventionally, how-

ever, neutron reflectivity treats the dot product between the magnetic induction and neutron magnetic moment classically: $V_m = -\boldsymbol{\mu} \cdot \mathbf{B} = \pm |\boldsymbol{\mu}| |\mathbf{B}| \cos(\theta)$, where θ is the angle between the incoming neutron polarization direction and the direction of the magnetization inside the film. Writing the magnetic potential as a classical dot product implies that the neutron energies in the magnetic layer have a continuous distribution from $-|\boldsymbol{\mu}| |\mathbf{B}|$ to $+|\boldsymbol{\mu}| |\mathbf{B}|$. This predicts that the critical angle for total reflection depends on the angle between the direction of polarization and the direction of the magnetic field inside the layer:

$$\frac{4\pi \sin(\alpha_c^\pm)}{\lambda} = Q_c^\pm = \sqrt{\frac{2m}{\hbar^2} (V_n \pm |\boldsymbol{\mu}| |\mathbf{B}_s| \cos(\theta))}, \quad (1)$$

where α is the glancing angle to the surface, λ is the wavelength of the neutrons, and Q_c^\pm is the critical scattering vector. There are experimental data [11, 13] on magnetic multilayers which apparently confirm this behavior. Therefore, the classical representation appears to provide a convenient and transparent way to describe the experimental observations [9, 10, 11, 12].

From the Stern-Gerlach experiment we know that there are only two eigen states for the spin 1/2 particles in a magnetic field. Therefore, the eigen wave number of a neutron in a magnetic thin film has two proper values. After solving the Schrodinger equation one obtains two eigen wave numbers for neutrons in a magnetic film: $k_\pm^2 = \frac{2m}{\hbar^2} (V_n \pm |\boldsymbol{\mu}| |\mathbf{B}|)$. They correspond to two possible states of spin orientation: one for the case, when the spin is parallel to the magnetic induction, and the other one for the antiparallel orientation. It follows that there are only two possible energies and consequently only two values for the index of refraction corresponding to the spin-up and spin-down states of the neutrons. Therefore,

QM predicts that there are only two critical angles for the total reflection: one corresponding to the R^+ and one to the R^- reflectivity

$$\frac{4\pi \sin(\alpha_c^\pm)}{\lambda} = Q_c^\pm = \sqrt{\frac{2m}{\hbar^2} (V_n \pm |\mu| |B_s|)} \quad (2)$$

Obviously there is a contradiction between the quantum mechanical prediction (Eq.2) and the prediction based on the classical representation of the magnetic potential (Eq.1): quantum mechanics predicts that the spin states of the neutron is determined by the magnetic induction in the sample, whereas classical representation of the magnetic potential, supported by experiments on magnetic multilayers, assert that the spin states of the neutrons is fixed by the incident polarization axis.

Here we describe an experiment which provides direct and unambiguous evidence for the spin states of neutrons in magnetic media. The goal is to find a system where the angle between the neutron polarization and direction of the magnetization inside of the film can be fixed and controlled. Then we measure the R^+ and R^- reflectivities and determine whether the position of the critical edges changes as a function of the angle θ , or whether the critical edges stay fixed, and only intensity redistributes between reflections R^+ and R^- with change of θ . The easiest way to control the angle θ is to rotate the magnetic film and therefore the magnetization direction with respect to the neutron spin polarization, which remains fixed in space outside of the sample. This requires that the film should have a high remanent magnetization. Additionally, the film thickness should exceed the average neutron penetration depth [15]. The last requirement is essential in order to avoid neutron tunnelling effects which will hinder the precise determination of the critical edges.

SAMPLE CHARACTERIZATION BY MOKE AND PNR

To fulfill the aforementioned requirements, we have chosen a 100 nm thick polycrystalline Fe film deposited by rf-sputtering on a Si substrate. The thickness of the Fe films was about 4 times larger than the average penetration depth $1/\sqrt{2mV_N/\hbar^2}$. The Fe film was covered with thin Co and CoO layers, the latter one protecting the Fe film from oxidation. For sample characterization at room temperature we first recorded hysteresis loops with the magneto-optical Kerr effect (MOKE). A series of hysteresis loops were taken with the field parallel to the film plane but with different azimuth angles of the sample. A typical hysteresis loop is shown in Fig. 1. The coercive field is about 20 Oe and the remanence is high. A plot of the ratio between the remanent magnetization and saturation magnetization M_{rem}/M_{sat} versus the rotation angle about the sample normal is shown in

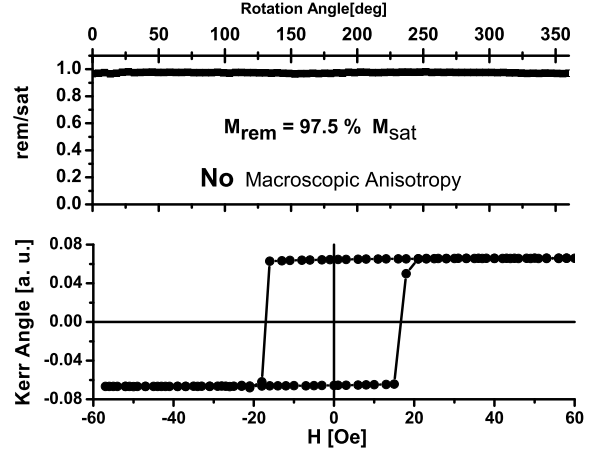


FIG. 1: Bottom: hysteresis loop of the polycrystalline Fe/Si sample measured by MOKE. Top: the behavior of the remanent magnetization as a function of the rotation angle extracted from hysteresis loops.

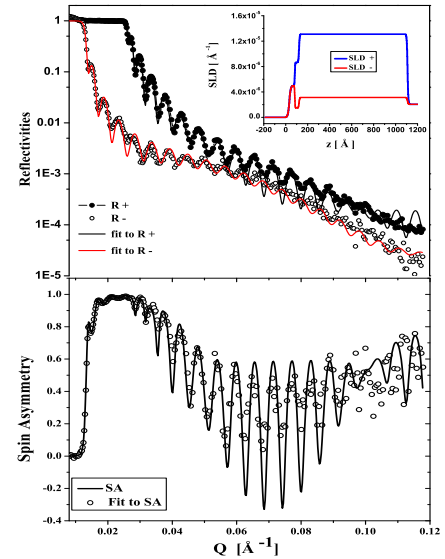


FIG. 2: (Color online). Top: Polarized neutron reflectivity curves R^+ (solid black circles) and R^- (open black circles) of the Fe/Si sample. The black line is the simulated R^+ reflectivity and the red (light gray) line is the simulated R^- reflectivity. The applied magnetic field was 2000 Oe. In the inset, the magnetic profile obtained from fitting the data is shown. Bottom: Experimental (open black symbols) and simulated (black line) spin asymmetry $((R^+ - R^-)/(R^+ + R^-))$ are plotted for the same sample in saturation. All lines in the top and bottom panels are fits to the data points using the GMM (for more details see text). The abscissa is the wave vector transfer: $Q = 4\pi \sin(\alpha)/\lambda$.

Fig. 1. We conclude that the system has no macroscopic anisotropy and the remanent magnetization is 97.5% of the saturation magnetization.

Neutron reflectivity experiments were performed using the angle dispersive neutron reflectometer ADAM installed at the Institut Laue-Langevin, Grenoble, which operates at a fixed wavelength of 4.41 Å. The R^+ and R^- reflectivities and the spin asymmetry $(R^+ - R^-)/(R^+ + R^-)$ in a saturation field of 2000 Oe are plotted in the top and bottom panel, respectively, of Fig. 2. The solid lines are fits to the data points using the *PolarFit* code based on the general matrix method (GMM) [7]. The fit and sample parameters are listed in Table I. In order to obtain a high confidence of the fit parameters, all reflectivities were fitted together and with the same parameter set. In general it is useful to fit first the spin asymmetry, for which geometrical and normalization parameters drop out.

TABLE I: Parameters of the Fe/Si sample obtained by fitting to the R^+ and R^- data shown in Fig. 2. d is the layer thickness, σ is the rms roughness, SLD is the scattering length density, and B is the magnetic induction in the ferromagnetic films.

Layer	d [Å]	σ [Å]	SLD	B [Oe]
$\text{Co}_y\text{O}_{1-y}$	50	11.5	4.99e-6	0
$\text{Co}_x\text{Fe}_{1-x}$	39	3	5.0518e-6	15563.4
Fe	987	5	8.024e-06	21600
substrate	non	6	2.073e-06	0

From Table I and the magnetic characterization (Fig. 1) we conclude that the sample fulfills the requirements as concerns thickness, anisotropy, and remanence as required for our experiment.

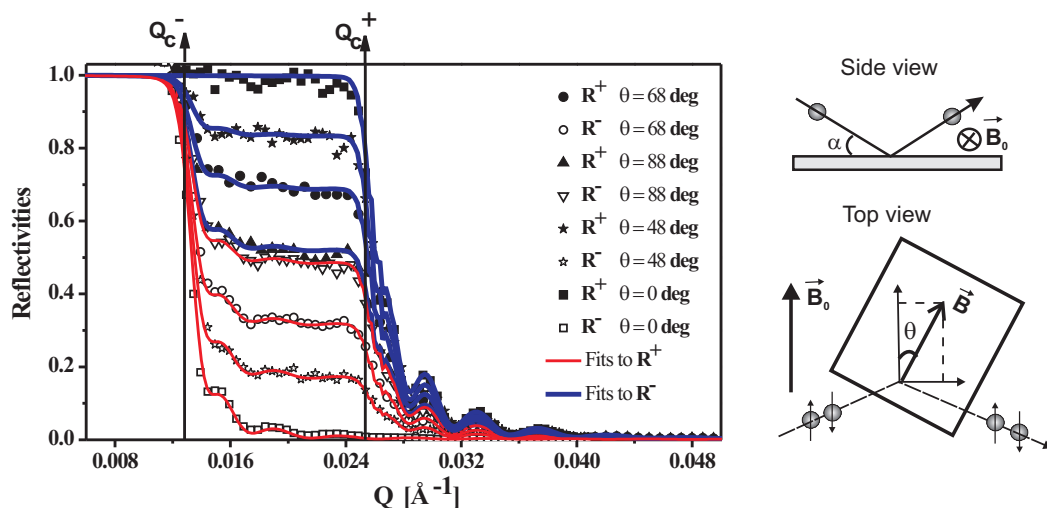


FIG. 3: (Color online). Experimental (symbols) and simulated (lines) reflectivity curves (R^+ and R^-) from Fe(1000 Å)/Si sample. The abscissa is the wave-vector transfer. The two sets of R^+ (solid black symbols) and R^- (open black symbols) reflectivity curves were measured for four different θ angles between the neutron polarization along \mathbf{B}_0 and the direction of the magnetic induction (\mathbf{B}) which lies in the sample plane. The guiding field is $B_0 \approx 10$ Oe. The blue (thick dark gray) lines are the simulated R^+ reflectivities and the red (thin light gray) lines are the simulated R^- reflectivities. In the right side the experimental geometry is shown. The figure shows that the critical edges Q_c^+ and Q_c^- are not sensitive to the θ angle.

ROTATION EXPERIMENT

The rotation experiment was performed as follows: the Fe layer was magnetized parallel to the neutron polarization direction and then the magnet was removed. A small guiding field (H_c) is still present at the sample position in order to maintain the neutron polarization. Subsequently a series of R^+ and R^- reflectivities, shown in Fig. 3, were measured for several in-plane rotation angles of the sample. We observe two characteristics of the

reflectivities: (1) the critical edges are fixed and independent of the in-plane rotation angle θ (see Eq. 2), and (2) the R^- intensity continuously increases at the expense of the R^+ intensity as a function of the θ angle. Using the parameters obtained from the fit to the saturation data (see Table I) and using the rotation angle θ as set during the experiment, we have simulated [14] the reflectivities using the GMM approach [7] which transparently predicts the behavior of the critical edges described by Eq. 2. The simulated curves are plotted together with the

experimental data in Fig. 3. There are no free parameters for these simulations, providing an excellent description of the experimental results. The fixed critical edges Q_+^c and Q_-^c can easily be interpreted in the context of the neutron spin states in homogenous magnetic media as discussed in the introduction.

EXPERIMENTAL DETERMINATION OF MAGNETIZATION ORIENTATION

The sensitivity to the in-plane rotation angle of the magnetization is seen very clearly in the reflected intensities R^+ and R^- plotted in Fig. 3. It has been shown theoretically [16] that, for a single magnetic layer, the normalized spin asymmetry ($nSA(\theta)$) is directly related to the θ angle through the following expression:

$$nSA(\theta) = \frac{SA(\theta)}{SA(0)} = \cos(\theta) \quad (3)$$

Now, we use our experimental data shown in Fig. 3 to confirm the validity of this equation. In Fig. 4 is shown the experimental normalized spin asymmetry and the cosine of the experimental angles. The agreement between the experimental normalized spin asymmetry (symbols) and the cosine of the θ angles (lines) set during the experiment is excellent over the whole wave vector transfer range. It follows that the magnetization orientation of a single magnetic layer with respect to the neutron polarization outside the layer can be easily extracted experimentally using Eq. 3. For more complicated systems a numerical fitting is still necessary. The nSA is an important measure of hysteresis loops. It was shown in Ref. [16] that nSA can be written, generally, as: $nSA = M_{||}/M_{sat}$ for both, magnetization reversal via coherent rotation and via domain wall movement. This implies that nSA reproduces the hysteresis loops as measured by SQUID or MOKE. Here we confirm the validity of the nSA for determining the magnetization reversal via coherent rotation. We mention that this equation is valid for samples which contain a single magnetic layer. Comparing MOKE or SQUID hysteresis loops with nSA is a very useful tool for the evaluation of magnetic domain state and/or a reduced magnetization within the layer.

MULTILAYERS

Our next topic is to investigate the neutron spin states in multilayers with noncollinear magnetization of adjacent layers. We simulated the reflectivity profile of a $[\text{Fe}(60\text{\AA})/\text{Cr}(8\text{\AA})]_{40}/\text{Si}$ superlattice, with thicknesses of the Fe and Cr layers which are typical for many real superlattices [13]. For the simulation we used the free-ware code *PolarSim* [14] based on GMM for the calcula-

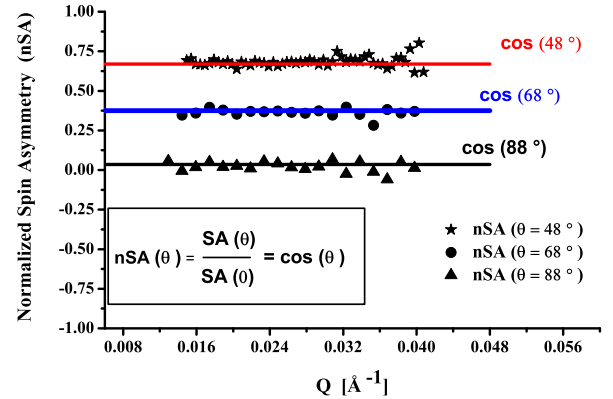


FIG. 4: (Color online). Solid black symbols: The experimental normalized spin asymmetries ($nSA(\theta) = SA(\theta)/(SA(0))$), plotted as a function of the wave-vector transfer Q . Lines: The three lines are the cosines of the corresponding angles set during the experiment. From top: cosine of 48° (thin gray (red) line), 68° (thick gray (blue) line), and 88° (thin black line), respectively. The angles are the experimental rotation angles θ used during the experiment shown in Fig. 3. The experimental normalized spin asymmetries are assembled from the R^+ and R^- reflectivities shown in Fig. 3. This figure shows that the equation $nSA(\theta) = \cos(\theta)$ is valid over the whole Q range for a single magnetic layer. It can be used to extract the angle θ directly from the experimental reflectivities.

tion of the reflection and transmission coefficient together with a full quantum mechanical description of the spin states [7]. In the simulation the choice of a Si substrate has the advantage that it does not obscure the critical edge of the (-) neutron state. In the top panel of Fig. 5 we show simulations of R^+ and R^- reflectivities for three angles γ between the magnetization vectors of adjacent Fe films: $\gamma = 0$ (or ferromagnetic alignment); $\gamma = 100^\circ$; and $\gamma = 170^\circ$ (close to antiferromagnetic alignment). Our focus is on the behavior of the critical scattering vector for total reflection. We observe that for $\gamma = 0$ the (+) and (-) critical scattering vectors are well separated and that they contain information about the saturation magnetization. When the γ value increases, the critical edges approach each other. For an angle $\gamma = 180^\circ$ (not shown here) there is no difference between the R_+ and R_- reflectivities. The main result from this simulation is the observation that the separation of the critical edges is a continuous function of the angle γ between the in-plane adjacent magnetization vectors. The critical edge positions satisfy the following relation:

$$\frac{4\pi \sin(\alpha_c^\pm)}{\lambda} = Q_c^\pm = \sqrt{\frac{2m}{\hbar^2} (V_n^{eff} \pm |\mu||\mathbf{B}_s| \cos(\gamma/2))}, \quad (4)$$

where V_n^{eff} is an effective nuclear potential. Clearly, for this geometry the angles θ and $\gamma/2$ coincide if the neutron

polarization is parallel to the average field $(\mathbf{B}_1 + \mathbf{B}_2)/2$, where B_1 and B_2 are the magnetic field inductions of adjacent layers. Therefore, numerically, the eqs. 1 and 3 are almost identical. However, there is a fundamental difference: similarly to the single layer, the θ angle does not influence the position of critical edges, whereas the γ angle is solely responsible for the continuous shift.

To shed more light on how the θ and γ angles affect the critical edges for polarized neutron reflectivity at the multilayers we simulated numerically the rotation experiment performed on the single layer. For a fixed coupling angle of $\gamma = 90^\circ$, as it can be achieved also experimentally via biquadratic exchange coupling, the reflectivities R^+ and R^- are plotted as a function of the θ angle. Here the θ angle is the angle between the incoming neutron polarization and the direction of the average magnetization vector of two adjacent ferromagnetic layers. The results are shown in the bottom panel of Fig. 5. We observe a similar behavior of the critical edges and intensities as for the single layer. While the positions of the critical scattering vectors Q_+^c and Q_-^c remain fixed for a constant coupling angle γ , the R^- intensity increases on the expense of the R^+ intensity with increasing θ angle. With this simulations we lift the contradiction stated in the introduction by showing that Eq. 1 is a particular case of Eq. 4, which, in turn, is in agreement with the QM description of the neutron spin states in magnetic media Eq. 2. The different behaviors of the critical edges for the case of a single homogeneous ferromagnetic layer and for a multilayer with alternating directions of the layer magnetization vectors now becomes obvious: in the multilayer the neutrons are affected by an average magnetic potential which depends on the relative orientation of the magnetic induction in the individual layers. However, in both cases, single film as well as multilayer, the magnetic potential of the individual layers ($V_m = |\mu||\mathbf{B}_s|$) enters the algorithm for calculating the reflectivities.

It should be noted that the dependence of Q_+^c and Q_-^c on the angle γ in a multilayer is a general property of the periodic potential with different field orientation and magnitude. It is natural to expect that such a sample is a noncollinear ferrimagnet with ferromagnetic field $\mathbf{B}_f = (\mathbf{B}_1 + \mathbf{B}_2)/2$,

$$B_f = |\mathbf{B}_1 + \mathbf{B}_2|/2 = B \cos(\gamma/2), \quad (5)$$

and with antiferromagnetic field $B_{af} = (\mathbf{B}_1 - \mathbf{B}_2)/2$,

$$B_{af} = |\mathbf{B}_1 - \mathbf{B}_2|/2 = B \sin(\gamma/2). \quad (6)$$

Then, the critical edges can be expected to be given by Eq. 4.

To further stress the origin of the effective nuclear potential V_n^{eff} term in Eq. 4., let us consider the critical edge for non-polarized neutrons when scattered at a $[\text{Fe}(x \text{ \AA})/\text{Cr}(y \text{ \AA})]_\infty$ multilayer. Naively, we may expect that the critical edge to be given by the Fermi interaction potential of Fe as it is higher than the potential of Cr. This

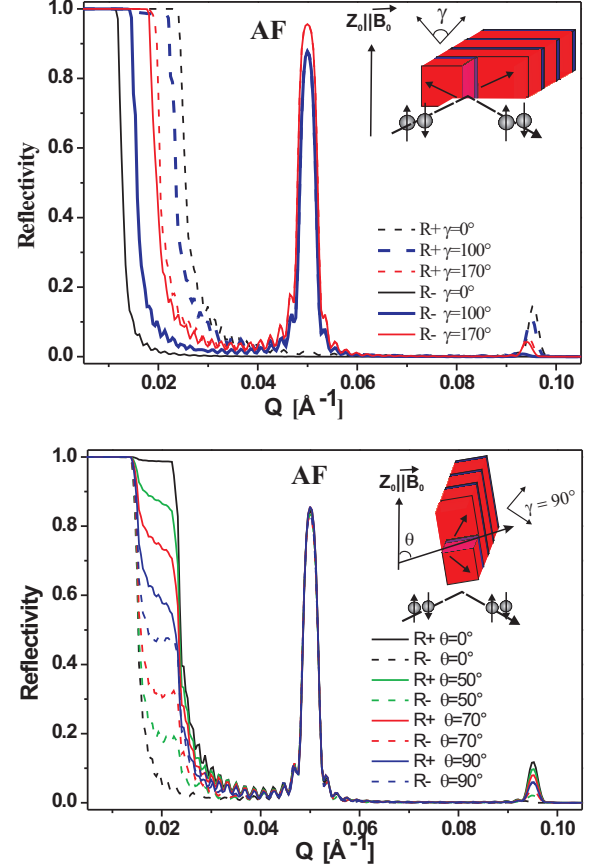


FIG. 5: (Color online). Top: Simulation of polarized neutron reflectivities [R^+ (dashed lines, shifting from right to left), R^- (solid lines, shifting from left to right)] for a Fe/Cr multilayer as a function of coupling angle (γ) between the magnetization vectors of adjacent Fe layers. Bottom: Simulations of R^+ (solid lines, shifting from top down) and R^- (dashed lines, shifting from bottom up) as a function of rotation angle θ for $\gamma = 90^\circ$.

is, however, not the case. For a finite thickness x of the Fe layer and zero thick Cr layer, indeed the critical edge is equal to the critical edge of a single thick Fe layer. Vice versa, for zero thickness of Fe layer and finite thickness y for the Cr layer the critical edge is given by the Fermi potential of Cr. However, when both layers have finite thicknesses the critical edge of the multilayer will vary from the value for pure Fe to the value for pure Cr. Therefore, the critical edge for non-polarized neutrons reflected from a multilayer not only depends on the Fermi potential of the two separate layers, but also on their individual thicknesses.

CONCLUSIONS

In summary, we have analyzed the behavior of the critical scattering vectors Q_+^c and Q_-^c for total external reflection of a polarized neutron beam for the case of homogeneous ferromagnetic films and for antiferromagnetically coupled multilayers. For a single film we have observed experimentally and shown theoretically that the critical edges do not change as a function of the angle between the neutron polarization and the direction of the magnetic spins inside the film. They fulfill the relation Eq. 2: $Q_c^\pm = \sqrt{\frac{2m}{\hbar^2}} (V_n \pm |\mu||\mathbf{B}_s|)$, which directly reflects the spin states of the neutron beam in magnetic thin films. For multilayers we found that the critical edges for total external reflection move towards each other as a function of the coupling angle. Their position is well reproduced by the Eq. 4: $Q_c^\pm = \sqrt{\frac{2m}{\hbar^2}} (V_n^{eff} \pm |\mu||\mathbf{B}_s| \cos(\gamma/2))$. The $\cos(\gamma/2)$ dependence is not related to the neutron spin states in the magnetic media, but it is the result of the presence of a ferromagnetic field direction along the average field in the noncollinear ferrimagnetic. By choosing a fixed coupling angle γ between the magnetization vectors of adjacent layers and rotating the sample, the critical edges behave again in accordance with the neutron spin states in homogeneous magnetic media. Practically, the coupling angle in non-collinear superlattices can be inferred directly from the experimental data through the separation of the critical edges. For a single layer the orientation of the magnetization can be extracted experimentally from the spin asymmetry.

This work was supported by the Deutsche Forschungsgemeinschaft through the research network (SFB 491): *Magnetic heterostructures*, which is gratefully acknowledged. We would like to thank Sabine Erdt-Böhm for the sample preparation. The ADAM reflectometer is supported by BMBF contract O3ZA6BC1.

- [9] G.P. Felcher, R.O. Hilleke, R.K. Crawford, J. Haumann, R. Kleb, G. Ostrowski, Rev. Sci. Instrum. **58**, 609 (1987).
- [10] K. Temst, M.J. Van Bael, J. Swerts, H. Loosvelt, E. Popova, D. Buntinx, J. Bekaert, C. Van Haesendonck, Y. Bruynseraede, R. Jonckheere, H. Fritzsche, Superlattices and Microstructures **34**, 87-105 (2003).
- [11] C.F. Majkrzak, Physica B **221**, 342 (1996); Physica B **156**, 619 (1989).
- [12] H. Zabel, Physica B **198**, 156 (1994).
- [13] A. Schreyer, F. Ankner, T. Zeidler, H. Zabel, M. Schafer, J. A. Wolf, P. Grünberg, C. F. Majkrzak, Phys. Rev. B **52**, 16066 (1995).
- [14] Polarized Neutron Reflectivity Software (*PolarSim*), <http://www.ep4.rub.de/~radu/welcome/polar.html>
- [15] D. Bally, S. Todoreanu, S. Ripeanu, and G. Belloni, Rev. Sci. Instr. **33** (9), 916, (1962).
- [16] F. Radu, M. Etzkorn, R. Siebrecht, T. Schmitte, K. Westerholt, H. Zabel, Phys. Rev. B **67**, 134409 (2003).

* Electronic address: florin.radu@rub.de;
URL: <http://www.ep4.ruhr-uni-bochum.de>

- [1] E. Fermi and W. Zinn, Phys. Rev. **70**, 103 (1946) ;
- [2] D. J. Hughes, M. T. Burgy, Phys. Rev. , **81**, 498 (1951).
- [3] V. K. Ignatovich, Pis'ma JETP **28**, 311 (1978).
- [4] G. P. Felcher, Phys. Rev. B **24**, R1595 (1981).
- [5] M.R. Fitzsimmons, S. D. Bader, J. A. Borchers, G. P. Felcher, J. K. Furdyna, A. Hoffmann, J.B. Kortright, Ivan K. Schuller, T.C. Schulthess, S. K. Sinha, M. F. Toney, D. Weller, S. Wolf, J. Magn. Magn. Mater. **271**, 103 (2004).
- [6] N. K. Pleshanov, Z. Phys. B **94**, 233 (1994); Z. Phys. B **100**, 423 (1996).
- [7] F. Radu, V. K. Ignatovich, Physica B **267-267**, 175 (1999).
- [8] G. P. Felcher, S. G. E. te Velthuis, Appl. Surf. Sci. **182**, 209 (2001).